Distinguishing thermodynamics and spectroscopy for octupolar U(1) spin liquid of Ce pyrochlores

Gang Chen ⬡

International Center for Quantum Materials, School of Physics, Peking University, Beijing 100871, China;
Department of Physics and HKU-UCAS Joint Institute for Theoretical
and Computational Physics at Hong Kong, The University of Hong Kong, Hong Kong, China;
and Collaborative Innovation Center of Quantum Matter, Beijing 100871, China

Inspired by the progress on the spin liquid candidates $Ce_2Sn_2O_7$ and $Ce_2Zr_2O_7$ where the Ce ions carry the dipole-octupole doublets, we analyze the distinction between the thermodynamic and spectroscopic measurements for the octupolar U(1) spin liquid. Due to the peculiar properties of octupolar U(1) spin liquid and the selective Zeeman coupling, both uniform susceptibility and the spectroscopic measurements only probe the spinon excitations, while the specific heat measures all excitations. After clarifying the contents in each measurement, we observe that, thermodynamics carries the information of single spinon, while the spectroscopy is associated with spinon pairs. Such distinction immediately leads to the multiplicity relation of the excitation gaps from different measurements that include the uniform susceptibility, Knight shift, and $1/T_1$ spin lattice relaxation of NMR and μSR, and the inelastic neutron scattering measurements. We hope this work provides a useful recipe for the identification of fractionalization in the octupolar U(1) spin liquid and other spin liquids.

I. INTRODUCTION

Deconfinement and fractionalization have played an important role in our understanding of elementary excitations in the deconfined phases such as the one-dimensional spin chains and the high-dimensional topological states and spin liquids [1,2]. In weakly coupled spin chains with spin-1/2 local moments, the deconfined spinons can propagate within the chains and can only propagate in pairs between chains [3]. In high-dimensional deconfined phases such as topological states and spin liquids, the fractionalized excitations are deconfined in all spatial dimensions [1,2], and thus fundamentally modify the thermodynamic and dynamic properties of the systems. The detection and manipulation of these fractionalized and deconfined quasiparticles has become one of the central questions in modern condensed matter physics. In this work, we attempt to make use of the bare property of deconfinement to analyze the thermodynamics and spectroscopic properties for the pyrochlore U(1) spin liquid [4]. In particular, we focus on the octupolar U(1) spin liquid in the pyrochlore magnets with dipole-octupole local moments [5,6]. We hope to find sharp experimental evidence simply based on the deconfinement and fractionalization without invoking extra ingredients.

The rare-earth pyrochlore magnets [5–15] with the Nd^{3+} and Ce^{3+} ions and the rare-earth spinel magnets [16] such as $MgEr_2Se_4$ have been found to be the hosting materials for the dipole-octupole (DO) doublets. In particular, $Ce_2Sn_2O_7$

and $Ce_2Zr_2O_7$ exhibit the spin liquid behaviors [7,9–13], and more recent investigation has been applied to $Ce_2Hf_2O_7$ [17]. The DO doublet is a special Kramers doublet where each state of the doublet is a singlet representation of the D_{3d} point group [5]. In the specific case of $Ce_2Sn_2O_7$ and $Ce_2Zr_2O_7$ [7,9–13], although the Ce^{3+} ion has a total $J = 5/2$, the ground-state doublet of the crystal field has the wave function $|J^z = \pm \frac{3}{2}\rangle$ that is an integer multiple of $\frac{3}{2}$ for J^z and is thus a DO doublet where J^z is defined on the local 111 axis of each pyrochlore sublattice and will be omitted in the local-state expression below. The effective spin-1/2 moment, S, is then defined on the ground-state doublet with $S^z = \frac{1}{2}[|\frac{3}{2}\rangle\langle\frac{3}{2}| - |-\frac{3}{2}\rangle\langle-\frac{3}{2}|]$, $S^x = \frac{1}{2}[|\frac{3}{2}\rangle\langle-\frac{3}{2}| + |-\frac{3}{2}\rangle\langle\frac{3}{2}|]$, and $S^y = \frac{1}{2}[-i|\frac{3}{2}\rangle\langle-\frac{3}{2}| + i|-\frac{3}{2}\rangle\langle\frac{3}{2}|]$, where S^y transforms as a magnetic octupole and the remaining components transform as a magnetic dipole. The generic spin model for the DO doublets on the pyrochlore lattice is given as [5,6],

$$H = \sum_{\langle ij \rangle} J_y S_i^y S_j^y + J_x S_i^x S_j^x + J_z S_i^z S_j^z + J_{xz}\left(S_i^x S_j^z + S_i^z S_j^x\right)$$
$$- \sum_i \boldsymbol{h} \cdot \left(S_i^z \hat{z}_i\right), \tag{1}$$

where only the nearest-neighbor coupling is considered and a Zeeman coupling is introduced. Here due to the microscopic reason, only the S^z component couples linearly with the external magnetic field, and $\hat{z}_i$ is the local z direction (see Table I). The octupolar U(1) spin liquid is realized in the regime with the dominant and antiferromagnetic J_y coupling, and is a distinct symmetry-enriched U(1) spin liquid in three dimensions [5,6]. As a three-dimensional (3D) U(1) spin liquid, the octupolar U(1) spin liquid shares its universal properties such as the emergent quantum electrodynamics for

TABLE I. The local $\hat{z}$ directions of the four sublattices, and the four neighboring vectors that connect the tetrahedral centers.

μ	0	1	2	3
$\hat{z}_\mu$	$\frac{1}{\sqrt{3}}[111]$	$\frac{1}{\sqrt{3}}[1\bar{1}\bar{1}]$	$\frac{1}{\sqrt{3}}[\bar{1}1\bar{1}]$	$\frac{1}{\sqrt{3}}[\bar{1}\bar{1}1]$
$\hat{e}_\mu$	$\frac{1}{4}[111]$	$\frac{1}{4}[1\bar{1}\bar{1}]$	$\frac{1}{4}[\bar{1}1\bar{1}]$	$\frac{1}{4}[\bar{1}\bar{1}1]$

a 3D U(1) spin liquid with the elementary excitations such as the gapless photon, the magnetic monopole, and the spinon. The way the emergent electric and magnetic fields in the octupolar U(1) spin liquid are related to the physical spin operators, however, is fundamentally different from the conventional dipolar U(1) spin liquid. In the octupolar U(1) spin liquid, the emergent electric field is related to the octupole moment. More substantially, because the S^z operator flips the S^y component and creates the spinon-antispinon pair in the octupolar U(1) spin liquid, the selective Zeeman coupling in Eq. (1) implies that the magnetic measurement such as the inelastic neutron scattering measurement would only probe the spinon matter [6].

There were several attempts [18–22] including our earlier ones with other authors [6,8–10] that tried to establish the connection between the possible spin liquid state in the Ce pyrochlores and the spin liquid ground states for the DO doublets. The representative proposals were based on the spectroscopic ones or the thermodynamic fitting, and are closely related to the existing experiments. The octupolar U(1) spin liquid seems promising for these Ce pyrochlores. In this work, we attempt to make a clear distinction between the thermodynamic and the spectroscopic measurements for the octupolar U(1) spin liquid with the DO doublets on the pyrochlore magnets. We were partly inspired by the recent results of the thermodynamics on the Ce-pyrochlore in Ref. [22]. Due to the chosen question, this work will begin with the physical explanation and experimental clarification, and then be supplemented with more concrete calculation.

Historically, the distinction in the thermodynamic and the spectroscopic measurements was crucial in the seminal example of fractional quantum Hall effects and represents an important outcome of the quantum number fractionalization and the deconfinement [23]. For the $\nu = 1/3$ Laughlin state, the specific heat has an activated behavior at low temperatures, and the activation gap in the thermodynamics is essentially the gap of the Laughlin quasiparticle, Δ_l. This is because the low-temperature specific heat probes the gas of the deconfined Laughlin quasiparticles. In contrast, the electron spectral function also gives a gap, and this electron spectral gap Δ_e is simply three times the gap of the Laughlin quasiparticle with $\Delta_e = 3\Delta_l$. This remarkable result occurs because one single electron excites three Laughlin quasiparticles in the $\nu = 1/3$ fractional quantum Hall liquid. Thus, an analogous behavior for the octupolar U(1) spin liquid would be quite useful to identify the deconfined and fractionalized quasiparticles. This seems to be difficult because there are three different quasiparticles in the octupolar U(1) spin liquid and all of them may contribute to the measurements whereas there only exists one type of Laughlin quasiparticle in the $\nu = 1/3$ Laughlin state. Remarkably, as we will elaborate in this work, the unique

properties of the octupolar U(1) spin liquid and the DO doublet may potentially make this goal feasible experimentally. In addition, we discuss the response of the system in the magnetic fields in both weak field regime and the strong field regime.

The remaining parts of the paper are organized as follows. In Sec. II, we explain the thermodynamic properties, especially the spinon gap in the local magnetic susceptibility. In Sec. III, we turn to the spectroscopic measurements and emphasize the behavior of two-spinon gaps in the magnetic fields along different directions. In Sec. IV, we explain the magnon gaps and the magnon presence for the strong field limit, and especially the emergent properties for the field along the 110 direction. In Sec. V, we discuss various experimental aspects and the application to other systems.

II. THERMODYNAMICS

We start with the simplest thermodynamic property, i.e., the specific heat. The specific heat probes all the excitations that include the gapless gauge photon, the gapped magnetic monopoles, and the gapped spinons. While the gapless gauge photon gives a T^3 specific heat with an anomalously large coefficient [24], this behavior appears at very low temperatures and is very hard to be observed experimentally. The gapped magnetic monopole has a similar energy scale as the gauge photon and contributes to the specific heat in an activated fashion. The gapped spinon appears at a higher energy, and also contributes to the specific heat in an activated fashion. Due to the deconfined nature of the magnetic monopole and the spinon, the thermal activation of them at very low temperatures creates a dilute gas of both. The spinon experiences the magnetic monopole as the flux, and there exist statistical interactions between them. Moreover, the spinons (magnetic monopoles) interact with themselves with the Coulomb interaction due to the emergent electric (magnetic) charge that are carried by them. Because the thermal activation leads to a soup of three different excitations, it might be difficult to separately identify each contribution. Nevertheless, it is still important to emphasize that, in the dilute gas limit where the quasiparticle interactions can be neglected, the specific heat then probes the properties of individual particles. Thus, the activated contribution from the spinon gas simply reveals the gap and the density of states of the individual spinon. This is also true for the magnetic monopoles. If one is able to extract the activation gaps from the specific heat, the gaps would be associated with a single spinon or magnetic monopole. The above discussion leads to the following qualitative expression for the low-temperature specific heat:

$$C_v(T) \sim f_p T^3 + f_s e^{-\Delta_s/T} + f_m e^{-\Delta_m/T}, \qquad (2)$$

where Δ_s and Δ_m are the gap of single spinon and single magnetic monopole, respectively. Here f_p, f_s and f_m are the prefactors that depend on the properties such as the density of states for these quasiparticle excitations.

We now turn our attention to the other common thermodynamic quantity, i.e., the magnetic susceptibility. From Eq. (1), only the S^z component is linearly coupled to the magnetic field. Since S^z creates the spinon pair, then the low-temperature magnetic susceptibility is probing the

magnetic properties of the spinon gas in the dilute spinon regime. Thus, the thermal activation of spinons would show up in the magnetic susceptibility. On the other hand, for the spin-orbit-coupled systems where the continuous spin rotational symmetry is absent, the total magnetization is not a good quantum number to characterize the many-body quantum states [25]. Thus, the magnetic susceptibility in the zero-temperature limit is nonzero. To summarize, one expects that the low-temperature magnetic susceptibility behaves like

$$\chi \sim \chi_0 + g_s e^{-\Delta_s/T}, \tag{3}$$

where χ_0 is the constant zero-temperature magnetic susceptibility, and g_s is a prefactor that depends on the properties such as the spinon density of states. Experimentally, the above behavior is more suitable to be measured from the Knight shift in the NMR or μSR measurement. Since the NMR or μSR measurements are often performed at small and finite magnetic fields, the relation in Eq. (3) should be modified with the field. As long as the system remains in the spin liquid state, the gap Δ_s is the spinon gap except that this gap would be modified by the field, and χ_0 is replaced by the one in the field. The behavior of the spinon gap in the field will be explained in the later sections [6]. The generic expression of Eq. (3) should still hold at finite and small fields.

III. SPECTROSCOPIC MEASUREMENTS

How about the spectroscopic measurements? The spectroscopic measurement such as the inelastic neutron scattering is a data-rich measurement, and provides a lot of information about the excitation spectra including the dispersion, the density of states, and the spectral intensity. Again, due to the selective coupling with the S^z components, only the S^z-S^z dynamic spin structure factor is measured in the spectroscopic measurements [6,8]. Therefore, the inelastic neutron scattering and the $1/T_1$ spin lattice relaxation time measurements detect the two-spinon continuum. Thus, the spectral gap in the spectroscopic measurements directly reveals the gap of the two-spinon continuum. This spectral gap, Δ_c, is twice of the spinon gap Δ_s in Eq. (2) and Eq. (3) with

$$\Delta_c = 2\Delta_s. \tag{4}$$

This factor of 2 is an important consequence of fractionalization.

After the above qualitative physical explanation and reasoning, we turn to the more concrete calculation. In fact, the two-spinon continuum of the octupolar U(1) spin liquid with 0 flux or π flux was actually explored in our early work, but the questions that were addressed were about the spectral periodicity associated with the symmetry enrichment, the translation symmetry fractionalization, the field-modulated spinon dispersion, and Anderson-Higgs' transition [6,8]. So far, the existing experiments have not explored the continuous excitation from the perspective of the spectral periodicity. This was partly due to the experimental resolution.

The single spinon gap and excitation in the thermodynamic quantities were not paid much attention. Neither was the clear physical distinction between the thermodynamics and the spectroscopy. It is a bit illuminating for us to compare with the fractional quantum Hall context and to clarify the relation

between the single spinon gap from the thermodynamics and the spectral gap of the two-spinon continuum needs to be clarified.

We begin with the octupolar U(1) spin liquid with the 0 flux for the spinon matter and refer to it as octupolar U(1)$_0$ spin liquid. This state is realized in the regime where there exists a dominant and antiferromagnetic J_y coupling and the other exchanges are unfrustrated. For the sake of completeness, we here formulate the spinon dynamics from the microscopic spin model in this regime [6,8]. This formulation can be found in previous works [24], but addresses new questions in this work. For the purpose here, we consider a reduced model from Eq. (1) in this regime,

$$H_{\mathrm{OSL}} = \sum_{\langle ij \rangle} J_y S_i^y S_j^y - J_\perp (S_i^+ S_j^- + \mathrm{H.c.}) - \sum_i \boldsymbol{h} \cdot (S_i^z \hat{z}_i), \tag{5}$$

where $S_i^\pm \equiv S_i^z \pm iS_i^x$. This octupolar U(1)$_0$ spin liquid occurs for a predominant J_y coupling and unfrustrated transverse exchanges. To reveal the spinon-gauge coupling, we implement the well-known parton-gauge construction with

$$S_i^y = s_{\boldsymbol{rr}'}^y, \qquad S_i^+ = \Phi_{\boldsymbol{r}}^\dagger \Phi_{\boldsymbol{r}'} s_{\boldsymbol{rr}'}^+, \tag{6}$$

where $\Phi_{\boldsymbol{r}}^\dagger$ ($\Phi_{\boldsymbol{r}}$) creates (annihilates) a spinon at the tetrahedral center $\boldsymbol{r}$. These tetrahedral centers actually form a diamond lattice and are labeled by $\boldsymbol{r}, \boldsymbol{r}'$ to distinguish from the pyrochlore sites i, j. We have

$$H_{\mathrm{OSL}} = \sum_{\boldsymbol{r}} \frac{J_y}{2} Q_{\boldsymbol{r}}^2 - \sum_{\langle \boldsymbol{rr}' \rangle} \sum_{\langle \boldsymbol{r'r''} \rangle} J_\perp \Phi_{\boldsymbol{r}}^\dagger \Phi_{\boldsymbol{r}'} s_{\boldsymbol{rr}''}^+ s_{\boldsymbol{r''r'}}^-$$

$$- \sum_{\langle \boldsymbol{rr}' \rangle} \frac{1}{2} (\boldsymbol{h} \cdot \hat{z}_i)(\Phi_{\boldsymbol{r}}^\dagger \Phi_{\boldsymbol{r}'} s_{\boldsymbol{rr}'}^+ + \mathrm{H.c.}). \tag{7}$$

Here the operators $s^y, s^\pm$ refer to the emergent U(1) gauge fields such that $s_{\boldsymbol{rr}'}^y \simeq E_{\boldsymbol{rr}'}$ and $s_{\boldsymbol{rr}'}^+ \simeq 1/2 e^{iA_{\boldsymbol{rr}'}}$, and $Q_{\boldsymbol{r}} = \eta_{\boldsymbol{r}} \sum_\mu S_{\boldsymbol{rr}+\eta_{\boldsymbol{r}}\boldsymbol{e}_\mu}^y$ is imposed to enforce the physical Hilbert space, where $\eta_{\boldsymbol{r}} = +1(-1)$ for the I (II) sublattice and $\boldsymbol{e}_\mu'$s are the first neighboring vectors on the diamond lattice. Moreover, $Q_{\boldsymbol{r}}$ measures the electric charge density at $\boldsymbol{r}$ and thus satisfies $[\Phi_{\boldsymbol{r}}, Q_{\boldsymbol{r}'}] = \Phi_{\boldsymbol{r}}\delta_{\boldsymbol{rr}'}, [\Phi_{\boldsymbol{r}}^\dagger, Q_{\boldsymbol{r}'}] = -\Phi_{\boldsymbol{r}}^\dagger \delta_{\boldsymbol{rr}'}$.

For the octupolar U(1)$_0$ spin liquid, one sets $A_{\boldsymbol{rr}'} = 0$. The Hamiltonian in Eq. (7) is solved with the rotor approximation $\Phi_{\boldsymbol{r}} = e^{-i\phi_{\boldsymbol{r}}}$ where $|\Phi_{\boldsymbol{r}}| = 1$ and $[\phi_{\boldsymbol{r}}, Q_{\boldsymbol{r}'}] = i\delta_{\boldsymbol{rr}'}$. In the actual calculation, a Lagrangian multiplier is introduced to impose the unimodular constraint for $\Phi_{\boldsymbol{r}}$. The spinon dispersions are obtained as $\epsilon_\mu(\boldsymbol{k})$ where μ is the band index. For the octupolar U(1)$_0$ spin liquid, the translation symmetry is not fractionalized in a nontrivial way, and thus the spinon band number is essentially the sublattice number of the diamond lattice. Because the external magnetic field induces the intersublattice spinon tunneling in Eq. (7), the spinon bands are not degenerate. For the octupolar U(1) spin liquid when $J_\perp < 0$ is frustrated, a background π flux is experienced for the spinons. The U(1) spin liquid in this regime is referred to as the octupolar U(1)$_\pi$ spin liquid. One fixes the gauge to take care of the background π flux for the spinons, and the translation symmetry is fractionalized in a nontrivial way for the spinons. The spinons now have four bands. Throughout the calculation, we use the π flux for the spinons.
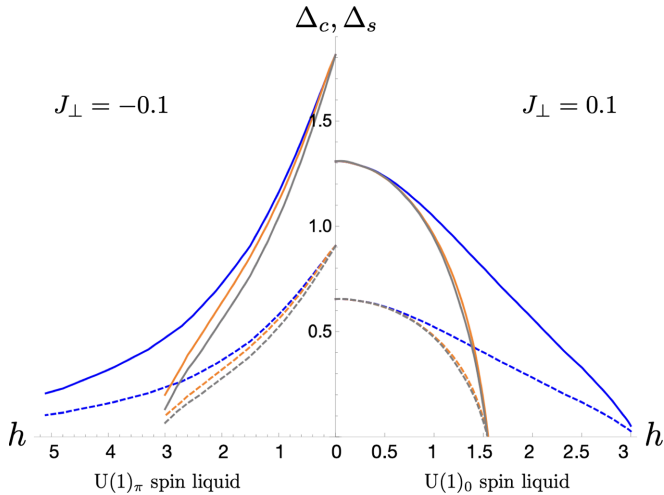
FIG. 1. The evolution of the spinon gaps with the magnetic fields of different directions for both $U(1)_0$ and $U(1)_\pi$ spin liquids. The left (right) panel is for the $U(1)_0$ [$U(1)_\pi$] spin liquid with $J_\perp = -0.1$ ($J_\perp = 0.1$). The solid (dashed) curve is the gap Δ_c (Δ_s) of the two-spinon continuum (single spinon). The gray, orange, and blue curves correspond to the magnetic field along 001, 111, and 110 directions, respectively. We have set $J_y = 1$.
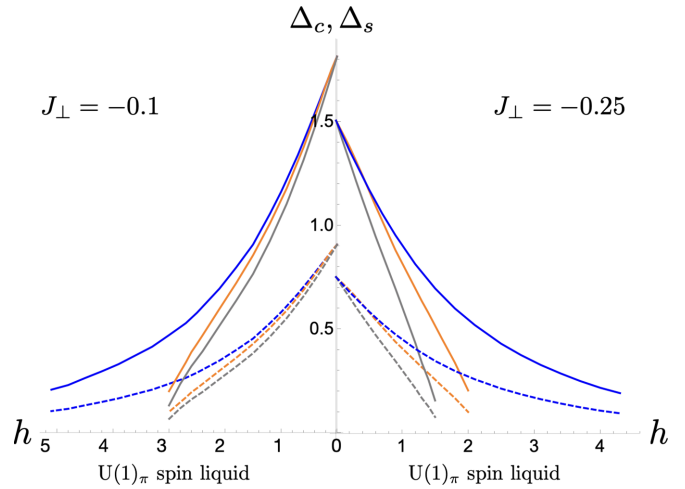

FIG. 2. The evolution of the spinon gaps with the magnetic fields of different directions for $U(1)_\pi$ spin liquid with different transverse couplings. The left (right) panel is for the $U(1)_\pi$ spin liquid with $J_\perp = -0.1$ ($J_\perp = -0.25$). The solid (dashed) curve is the gap Δ_c (Δ_s) of the two-spinon continuum (single spinon). The gray, orange, and blue curves correspond to the magnetic field along 001, 111, and 110 directions, respectively. We have set $J_y = 1$.

It is likely that, around the points where the spinon gap closes, the π flux state may give away to other competing states.

We label the spinon dispersions as $\epsilon_\mu(\boldsymbol{k})$ where $\mu = 1, 2$ [1,2,3,4] for the octupolar $U(1)_0$ [$U(1)_\pi$] spin liquid. The single spinon gap Δ_s and the gap Δ_c for the two-spinon continuum are given as

$$\Delta_s = \mathrm{Min}[\epsilon_\mu(\boldsymbol{k})], \tag{8}$$

$$\Delta_c = \mathrm{Min}[\epsilon_\mu(\boldsymbol{k}_1) + \epsilon_\nu(\boldsymbol{k}_2)]. \tag{9}$$

The above expressions work for both octupolar $U(1)_0$ and $U(1)_\pi$ spin liquids. For the octupolar $U(1)_\pi$ spin liquid, an off-set momentum from the gauge fixing can be added to Eq. (9). Nevertheless, because the spinon energy is invariant under the translation by this momentum, so Eq. (9) is sufficient.

We perform an involved calculation of the spinon gaps with the self-consistent gauge mean-field theory for a wide range of magnetic fields and exchange couplings, and obtain the dependence of the spinon gaps on these parameters. In Fig. 1, we plot the comparison of the spinon gaps for the octupolar $U(1)_0$ and $U(1)_\pi$ spin liquids (with the same $|J_\perp|$) in the magnetic fields along different directions. Several key features can be obtained from the plots in Fig. 1. First, the gap of the spinon continuum is twice of the single spinon gap. Second, the spin liquid state is more robust against the fields for the $U(1)_\pi$ spin liquid. This is clearly expected as the π flux is due to the more frustrated transverse exchange. Third, the spin liquid states are more stable when the field is along 110 direction. This is because the field only couples two sublattices of the pyrochlore lattice and thus is less effective compared to the fields along other directions. Fourth, the spinon gap monotonically decreases as the field increases for all directions. Although the field does not suppress the spin liquid ground state immediately, the influence of the spinon dispersion and the spinon gap is quite remarkable and is a

visible effect experimentally. The monotonically decreasing spinon gap contrasts strongly with the magnon gap behavior for the field-polarized states that we will explain later.

In Fig. 2, we further compare the spinon gaps for the octupolar $U(1)_\pi$ spin liquid with different $J'_\perp$s. According to Ref. [22], $J_\perp = -0.25J_y$ is expected to be more relevant for $Ce_2Zr_2O_7$. There are not much qualitatively differences for different $J'_\perp$s except that the gap is a bit smaller for large $|J_\perp|$.

IV. MAGNON GAPS IN THE STRONG FIELD REGIME

In the strong field regime, the spin liquid state will be destroyed, and the system becomes a field-induced polarized state. For the field-polarized states in the strong field limit, the states for the 001 and 111 fields are quite clear. The 001 field induces a $\boldsymbol{q} = 0$ two-in two-out dipolar spin ice state in the S^z components. The 111 field induces a $\boldsymbol{q} = 0$ one-in three-out spin state in the S^z components. These two states have been partially analyzed in Ref. [8]. Here we compute the magnon spectra and find that the magnon gaps for these two states *increase* monotonically with the field strength (see Fig. 3). Due to the polarization effect on the S^z component, the spectral weight of the magnons for these polarized states in the neutron scattering experiments should be strongly suppressed. The field-polarized state along the 110 field, however, is quite different from the above two field directions.

A. Hidden octupolar order in the 110 field

It turns out that the field-polarized state for the 110 field is quite special in the octupolar spin ice regime. It is shown below that, the remaining unpolarized sublattices experience a $\mathbb{Z}_2$ symmetry breaking and induce an internal hidden order in the octupole moment at $T = 0$. This spontaneous hidden octupolar order turns out to be a unique property for the
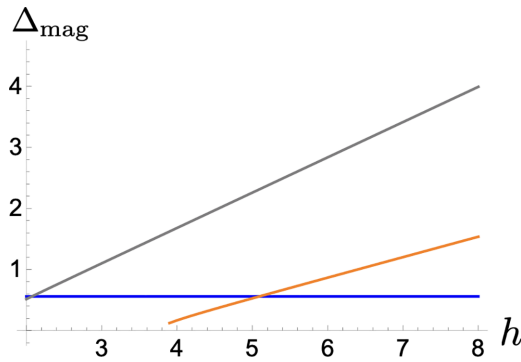
FIG. 3. The evolution of the magnon gap with the magnetic field in the strong field limit for the field-polarized states. The gray, orange, and blue curves correspond to the field along 001, 111, and 110 directions, respectively. The constant behavior of the magnon gap with the 110 field is explained in the main text. In the plot, we choose $J_y = 1$, $J_x = 0.75$, $J_z = 0.25$ that is compatible with the results in Ref. [22].

FIG. 4. The field-induced hidden ordered state for the 110 field. In the plot, the red arrows indicate the S^z configuration while the "+" and "−" refer to the S^y configuration due to the additional symmetry breaking on the unpolarized sublattices.

octupolar spin ice. Although the $\mathbb{Z}_2$ symmetry breaking on such chains along the unpolarized sublattices are independent, by assuming a $\mathbf{q} = 0$ state, we find that the magnon gap remains constant (see Fig. 3) and is mainly controlled by the octupolar coupling J_y.

Here we discuss the field-polarized states in the strong field limit. For the magnetic fields along 001 and 111 directions, since all the sublattices are coupled to the field with the Zeeman coupling, all the sublattices will be polarized by the field along their corresponding $+\hat{z}$ or $-\hat{z}$ directions. In particular, the 001 field induces a uniform two-in two-out spin state in the S^z components and the 111 field induces a three-in one-out spin state in the S^z components. The magnon gaps of these two polarized states grow as the field strength is increased (see Fig. 3). For the 110 field, however, only two sublattices are coupled to the field, and the other two sublattices do not directly experience the field.

In Table I, we have listed the local $\hat{z}$ directions for each sublattice. Under the 110 field, the zeroth sublattice is polarized in the $+\hat{z}$ direction, and the third sublattice is polarized in the $-\hat{z}$ direction. This is depicted as the red arrows in Fig. 4. The first and second sublattices are decoupled from the magnetic field. Moreover, the internal exchange field on the first and second sublattices from the polarized $\langle S^z \rangle$ of the zeroth and third sublattices is canceled, thus the first and second sublattices are effectively decoupled from the zeroth and third sublattices at the classical or mean-field sense. The magnetic state of the first and second sublattices will then be determined by the residual interaction. The first and second sublattices in fact form multiple chains along $1\bar{1}0$ directions. Since we are considering the system in the octupolar spin ice regime with a predominant J_y coupling, the interactions on these chains are dominated by the Ising interaction on the octupole S^y components, and these chains are effectively decoupled from each other in the classical sense. Even with the field, the Hamiltonian of the system is still invariant under the $\mathbb{Z}_2$ transformation,
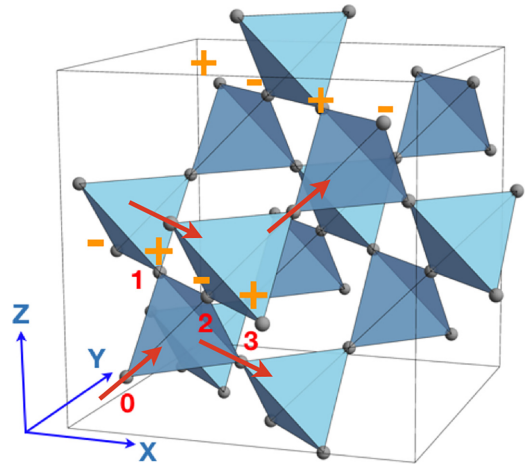
$$\mathbb{Z}_2 : S^y \rightarrow -S^y. \tag{10}$$

The predominant antiferromagnetic intrachain J_y coupling breaks this $\mathbb{Z}_2$ symmetry by creating an antiferromagnetic octupolar $\langle S^y \rangle$ order along the chains (see Fig. 4). Remarkably, the exchange field from the $\langle S^y \rangle$ configuration on the first and second sublattices is canceled on the zeroth and third sublattices. Thus, the antiferromagnetic octupolar order has no direct impact on the zeroth and third sublattices at the mean-field sense. As a result, the interchain coupling via the intermediate first and second sublattices is absent at the mean-field level. The antiferromagnetic octupolar order on each chain is then independent and has a twofold degeneracy on each chain.

To summarize, the antiferromagnetic octupolar $\langle S^y \rangle$ order on the $1\bar{1}0$ chains, which is actually a hidden order, arises from the predominant J_y coupling in the octupolar spin ice regime after polarizing the other two sublattices in S^z antiferromagnetically. Thus, it is one *unique* property of the octupolar spin ice.

B. Magnon excitation for the 110 field

What about the magnon excitations in the field-induced states for the 110 field? Apparently, there are two types of magnonlike excitations. One is from the flipping of $\langle S^z \rangle$ on the zeroth and third sublattices. The energy gap of these magnons is governed by the magnetic field and would grow with the magnetic field. The other type of magnon is from the flipping of $\langle S^y \rangle$ on the first and second sublattices. The energy gap of these magnons is governed by the J^y coupling and seems insensitive to the magnetic field. To demonstrate this, we perform an explicit spin-wave calculation.

We consider a $\mathbf{q} = 0$ state in Fig. 4 such that the octupolar order on the effectively decoupled $1\bar{1}0$ chains is related by lattice translations. The reason that we choose this simple state is for our convenience to do the spin-wave calculation, and the mean-field analysis does not have the interchain correlation of the antiferromagnetic octupolar order. We here adopt the thermodynamic result in Ref. [22] and consider the model spin Hamiltonian in Eq. (1) with

$J_y = 1$, $J_x = 0.75$, $J_z = 0.25$, $J_{xz} = 0$. In the linear spin-wave theory, we express the spin operators via the Holstein-Primakoff transformation. For the zeroth and third sublattices, we have

$$i \in 0, \quad S_i^z = \frac{1}{2} - a_i^\dagger a_i, \tag{11}$$

$$S_i^x = \frac{1}{2}(a_i + a_i^\dagger), \tag{12}$$

$$S_i^y = \frac{1}{2i}(a_i - a_i^\dagger), \tag{13}$$

$$i \in 3, \quad S_i^z = -\frac{1}{2} + b_i^\dagger b_i, \tag{14}$$

$$S_i^x = \frac{1}{2}(b_i + b_i^\dagger), \tag{15}$$

$$S_i^y = \frac{1}{2i}(b_i^\dagger - b_i), \tag{16}$$

and for the first and second sublattices, we have

$$i \in 1, \quad S_i^y = \frac{1}{2} - c_i^\dagger c_i, \tag{17}$$

$$S_i^z = \frac{1}{2}(c_i + c_i^\dagger), \tag{18}$$

$$S_i^x = \frac{1}{2i}(c_i - c_i^\dagger), \tag{19}$$

$$i \in 2, \quad S_i^y = -\frac{1}{2} + d_i^\dagger d_i, \tag{20}$$

$$S_i^z = \frac{1}{2}(d_i + d_i^\dagger), \tag{21}$$

$$S_i^x = \frac{1}{2i}(d_i^\dagger - d_i). \tag{22}$$

The linear spin-wave Hamiltonian is then given as

$$H_{\text{sw}} = \sum_{\boldsymbol{k}} \sum_{\mu\nu} \Psi_{\boldsymbol{k},\mu}^\dagger M_{\mu\nu}(\boldsymbol{k}) \Psi_{\boldsymbol{k},\nu}, \tag{23}$$

where $\Psi_{\boldsymbol{k},\nu} = (a_{\boldsymbol{k}}, b_{\boldsymbol{k}}, c_{\boldsymbol{k}}, d_{\boldsymbol{k}}, a_{-\boldsymbol{k}}^\dagger, b_{-\boldsymbol{k}}^\dagger, c_{-\boldsymbol{k}}^\dagger, d_{-\boldsymbol{k}}^\dagger)^T$, and $M_{\mu\nu}(\boldsymbol{k})$ is a 8×8 matrix with

$$M(\boldsymbol{k}) = \begin{bmatrix} A_{\boldsymbol{k}} & B_{\boldsymbol{k}} \\ B_{\boldsymbol{k}}^\dagger & A_{-\boldsymbol{k}}^* \end{bmatrix}. \tag{24}$$

Here both $A_{\boldsymbol{k}}$ and $B_{\boldsymbol{k}}$ are 4×4 matrices with

$$A_{\boldsymbol{k}} = \begin{bmatrix} \frac{1}{2}(J_z + h) & \frac{1}{4}(J_x - J_y)\cos(\boldsymbol{k} \cdot \boldsymbol{e}_{03}) & \frac{1}{4i}J_x \cos(\boldsymbol{k} \cdot \boldsymbol{e}_{01}) & -\frac{1}{4i}J_x \cos(\boldsymbol{k} \cdot \boldsymbol{e}_{02}) \\ \frac{1}{4}(J_x - J_y)\cos(\boldsymbol{k} \cdot \boldsymbol{e}_{03}) & \frac{1}{2}(J_z + h) & \frac{1}{4i}J_x \cos(\boldsymbol{k} \cdot \boldsymbol{e}_{13}) & -\frac{1}{4i}J_x \cos(\boldsymbol{k} \cdot \boldsymbol{e}_{23}) \\ -\frac{1}{4i}J_x \cos(\boldsymbol{k} \cdot \boldsymbol{e}_{01}) & -\frac{1}{4i}J_x \cos(\boldsymbol{k} \cdot \boldsymbol{e}_{13}) & \frac{1}{2}J_y & \frac{1}{4}(J_z - J_x)\cos(\boldsymbol{k} \cdot \boldsymbol{e}_{12}) \\ \frac{1}{4i}J_x \cos(\boldsymbol{k} \cdot \boldsymbol{e}_{02}) & \frac{1}{4i}J_x \cos(\boldsymbol{k} \cdot \boldsymbol{e}_{23}) & \frac{1}{4}(J_z - J_x)\cos(\boldsymbol{k} \cdot \boldsymbol{e}_{12}) & \frac{1}{2}J_y \end{bmatrix}, \tag{25}$$

$$B_{\boldsymbol{k}} = \begin{bmatrix} 0 & \frac{1}{4}(J_x + J_y)\cos(\boldsymbol{k} \cdot \boldsymbol{e}_{03}) & -\frac{1}{4i}J_x \cos(\boldsymbol{k} \cdot \boldsymbol{e}_{01}) & \frac{1}{4i}J_x \cos(\boldsymbol{k} \cdot \boldsymbol{e}_{02}) \\ \frac{1}{4}(J_x + J_y)\cos(\boldsymbol{k} \cdot \boldsymbol{e}_{03}) & 0 & -\frac{1}{4i}J_x \cos(\boldsymbol{k} \cdot \boldsymbol{e}_{13}) & \frac{1}{4i}J_x \cos(\boldsymbol{k} \cdot \boldsymbol{e}_{23}) \\ -\frac{1}{4i}J_x \cos(\boldsymbol{k} \cdot \boldsymbol{e}_{01}) & -\frac{1}{4i}J_x \cos(\boldsymbol{k} \cdot \boldsymbol{e}_{13}) & 0 & \frac{1}{4i}(J_x + J_z)\cos(\boldsymbol{k} \cdot \boldsymbol{e}_{12}) \\ \frac{1}{4i}J_x \cos(\boldsymbol{k} \cdot \boldsymbol{e}_{02}) & \frac{1}{4i}J_x \cos(\boldsymbol{k} \cdot \boldsymbol{e}_{23}) & \frac{1}{4i}(J_x + J_z)\cos(\boldsymbol{k} \cdot \boldsymbol{e}_{12}) & 0 \end{bmatrix}, \tag{26}$$

where $\boldsymbol{e}_{\mu\nu} = \frac{1}{2}(\boldsymbol{e}_\mu - \boldsymbol{e}_\nu)$. The spin-wave spectrum is obtained by solving H_{sw} with the bosonic Bogoliubov transformation. The lowest magnon gap is found to be

$$\Delta_{\text{mag}} = [(J_y - J_x)(J_y + J_z)]^{1/2}. \tag{27}$$

In the large J_y limit, $\Delta_{\text{mag}} \simeq J_y$ and is essentially governed by the intrachain coupling along the $1\bar{1}0$ chains.

How about the spectral intensity of the magnon excitations in the inelastic neutron scattering? For the polarized states with the 001 and 111 fields, the S^z components are fully polarized in the strong field limit. The spin operators that create magnon excitations are mainly S^x and S^y components that do not couple to the external fields at the linear level. Thus, the spectral intensity is expected to be gradually suppressed as the field is increased. The field-induced octupolar ordered state for the 110 field, however, behaves quite differently. Along the $1\bar{1}0$ chains, the system orders antiferromagnetically in S^y, and the S^z component that couples to the neutron spins works as a spin flipping operator for S^y and creates the magnon excitation. The spectral intensity of these intrachain magnons should be persistent even in the strong

field limit and is a signature of hidden order in the system [26–29].

V. DISCUSSION

A. More discussion about spinon gaps

The multiplicity relation between the thermodynamic gap from the Knight shift and the spectral gap from the inelastic neutron scattering or $1/T_1$ spin lattice relaxation time measurement is a sharp consequence of deconfinement and fractionalization. All the results in this work are about the energy gaps and did not invoke any information about the crystal momentum. Although high-quality single-crystal samples may be ideal, the observation of these results actually does not require the single crystal samples. Thus, the Knight shifts and the spin lattice relaxation $1/T_1$ of the NMR and μSR measurements as well as the inelastic neutron scattering can all be performed with the powder or polycrystalline samples, except that the analysis of the NMR and μSR results require the local structural information.

Since the NMR and μSR measurements are often performed with the magnetic field, so it is better not to apply very

strong magnetic fields to destroy the spin liquid. From the previous experiences, the spin liquid is more stable when the field is in the 110 direction. The proposed octupolar $U(1)_\pi$ spin liquid for the Ce pyrochlores is more stable in the field compared to $U(1)_0$ spin liquid. These all suggest the experimental feasibility for field measurements [30]. Moreover, the spinon gap decreases with the magnetic field while the magnon gap of the field-polarized state does not decrease with the field. This can be a sharp and important result to distinguish the spinon from the magnon of the candidate states.

B. Discussion of field-induced competing states

Here we give more discussion about the field-induced states for a generic magnetic field where every sublattice is coupled to field. In the octupolar $U(1)$ spin liquid, the background gauge flux is mainly controlled by the transverse exchange $J_\perp$ term via third-order perturbation theory that generates the ring exchange to control the background gauge flux [4]. The Zeeman coupling with the magnetic field alone enters the ring exchange via sixth-order perturbation. Thus the spin liquid state is more stable with the field perturbation compared to the $J_\perp$ exchange. Nevertheless, it is likely that, the $J_\perp$ exchange and the field favor different background flux. This flux frustration can happen in the octupolar $U(1)_\pi$ spin liquid with the field. Moreover, a generic magnetic field alone would favor a uniform spin state. The proximate ordered state out of the octupolar $U(1)_\pi$ spin liquid would enlarge the unit cell and break the translation symmetry. Thus the uniform polarized state is not connected with the octupolar $U(1)_\pi$ spin liquid with a continuous or nearly continuous transition. Either the system experiences a first order phase transition, or the system goes through an intermediate state. The upper-field phase boundary of the octupolar $U(1)_\pi$ spin liquid in Fig. 2 and the lower-field phase boundary of the polarized states in Fig. 3 are not precisely known in our work. We have used the gauge mean-field theory for the system inside the spin liquid state, and have used the conventional mean-field theory with spin-wave theory for the field-induced states. These are rather different mean-field approaches, so one cannot simply compare the mean-field energies from them and thus cannot obtain a phase diagram by combining these different approaches.

For the special field along 110 direction, without the transverse exchange and other interactions, this Zeeman coupling alone, that only acts on two sublattices, cannot generate the quantum tunneling between distinct spin ice configurations of the predominant J_y Ising coupling. Only with other exchange interactions, the system can generate quantum tunneling between distinct spin ice configurations. For other high-symmetry field directions, the Zeeman coupling alone could generate the quantum tunneling between distinct spin ice configurations. In our actual calculation for the spinon properties [6], we simply fix the background $U(1)$ gauge for the spinons according to the sign of the transverse exchange.

C. Discussion about other applications

One can extend the discussion to the pyrochlore $U(1)$ spin liquid with non-Kramers doublets. This can be potentially relevant for the pyrochlore magnets with the Pr^{3+} and Tb^{3+} ions that include for example $Pr_2Zr_2O_7$, $Pr_2Hf_2O_7$ and $Tb_2Ti_2O_7$ [31–35]. Here, the spinon does not obviously show up in the magnetic measurement. Instead, it is the gauge photon and magnetic monopole that contribute [36,37]. Separating the contribution of the photon and the magnetic monopole can be an obstacle. On the broad context, the experimental identification of fractionalized excitations and their nontrivial symmetry enrichment in spin liquids is an unresolved question. On the thermodynamic side, there has been some efforts to detect the fractional spin quantum number of the spinon in the kagomé spin liquid candidate [38]. More generally, the distinction of thermodynamics and different spectroscopy can be quite useful in fulfilling this task.

[1] L. Savary and L. Balents, Quantum spin liquids: A review, Rep. Prog. Phys. **80**, 016502 (2017).

[2] J. Knolle and R. Moessner, A field guide to spin liquids, Annu. Rev. Condens. Matter Phys. **10**, 451 (2019).

[3] M. Kohno, O. A. Starykh, and L. Balents, Spinons and triplons in spatially anisotropic frustrated antiferromagnets, Nature Phys. **3**, 790 (2007).

[4] M. Hermele, M. P. A. Fisher, and L. Balents, Pyrochlore photons: The $U(1)$ spin liquid in a $S = \frac{1}{2}$ three-dimensional frustrated magnet, Phys. Rev. B **69**, 064404 (2004).

[5] Y.-P. Huang, G. Chen, and M. Hermele, Quantum Spin Ices and Topological Phases from Dipolar-Octupolar Doublets on the Pyrochlore Lattice, Phys. Rev. Lett. **112**, 167203 (2014).

[6] Y.-D. Li and G. Chen, Symmetry enriched U(1) topological orders for dipole-octupole doublets on a pyrochlore lattice, Phys. Rev. B **95**, 041106(R) (2017).

[7] R. Sibille, E. Lhotel, V. Pomjakushin, C. Baines, T. Fennell, and M. Kenzelmann, Candidate Quantum Spin Liquid in the Ce^{3+} Pyrochlore Stannate $Ce_2Sn_2O_7$, Phys. Rev. Lett. **115**, 097202 (2015).

[8] X.-P. Yao, Y.-D. Li, and G. Chen, Pyrochlore U(1) spin liquid of mixed-symmetry enrichments in magnetic fields, Phys. Rev. Res. **2**, 013334 (2020).

[9] B. Gao, T. Chen, D. W. Tam, C.-L. Huang, K. Sasmal, D. T. Adroja, F. Ye, H. Cao, G. Sala, M. B. Stone, C. Baines, J. A. T. Verezhak, H. Hu, J.-H. Chung, X. Xu, S.-W. Cheong, M. Nallaiyan, S. Spagna, M. B. Maple, A. H. Nevidomskyy *et al.*, Experimental signatures of a three-dimensional quantum spin liquid in effective spin-1/2 $Ce_2Zr_2O_7$ pyrochlore, Nature Phys. **15**, 1052 (2019).

[10] B. Gao, T. Chen, H. Yan, C. Duan, C.-L. Huang, X. P. Yao, F. Ye, C. Balz, J. R. Stewart, K. Nakajima, S. Ohira-Kawamura,

G. Xu, X. Xu, S.-W. Cheong, E. Morosan, A. H. Nevidomskyy, G. Chen, and P. Dai, Magnetic field effects in an octupolar quantum spin liquid candidate, Phys. Rev. B **106**, 094425 (2022).

[11] R. Sibille, N. Gauthier, E. Lhotel, V. Porée, V. Pomjakushin, R. A. Ewings, T. G. Perring, J. Ollivier, A. Wildes, C. Ritter, T. C. Hansen, D. A. Keen, G. J. Nilsen, L. Keller, S. Petit, and T. Fennell, A quantum liquid of magnetic octupoles on the pyrochlore lattice, Nature Phys. **16**, 546 (2020).

[12] J. Gaudet, E. M. Smith, J. Dudemaine, J. Beare, C. R. C. Buhariwalla, N. P. Butch, M. B. Stone, A. I. Kolesnikov, G. Xu, D. R. Yahne, K. A. Ross, C. A. Marjerrison, J. D. Garrett, G. M. Luke, A. D. Bianchi, and B. D. Gaulin, Quantum Spin Ice Dynamics in the Dipole-Octupole Pyrochlore Magnet $Ce_2Zr_2O_7$, Phys. Rev. Lett. **122**, 187201 (2019).

[13] E. M. Smith, O. Benton, D. R. Yahne, B. Placke, R. Schäfer, J. Gaudet, J. Dudemaine, A. Fitterman, J. Beare, A. R. Wildes, S. Bhattacharya, T. DeLazzer, C. R. C. Buhariwalla, N. P. Butch, R. Movshovich, J. D. Garrett, C. A. Marjerrison, J. P. Clancy, E. Kermarrec, G. M. Luke *et al.*, Case for a $U(1)_\pi$ Quantum Spin Liquid Ground State in the Dipole-Octupole Pyrochlore $Ce_2Zr_2O_7$, Phys. Rev. X **12**, 021015 (2022).

[14] J. Xu, O. Benton, A. T. M. N. Islam, T. Guidi, G. Ehlers, and B. Lake, Order out of a Coulomb Phase and Higgs Transition: Frustrated Transverse Interactions of $Nd_2Zr_2O_7$, Phys. Rev. Lett. **124**, 097203 (2020).

[15] S. Petit, E. Lhotel, B. Canals, M. Ciomaga-Hatnean, J. Ollivier, H. Mutka, E. Ressouche, A. R. Wildes, M. R. Lees, and G. Balakrishnan, Observation of magnetic fragmentation in spin ice, Nat. Phys. **12**, 746 (2016).

[16] D. Reig-i-Plessis, S. V. Geldern, A. A. Aczel, D. Kochkov, B. K. Clark, and G. J. MacDougall, Deviation from the dipole-ice model in the spinel spin-ice candidate $MgEr_2Se_4$, Phys. Rev. B **99**, 134438 (2019).

[17] V. Porée, E. Lhotel, S. Petit, A. Krajewska, P. Puphal, A. H. Clark, V. Pomjakushin, H. C. Walker, N. Gauthier, D. J. Gawryluk, and R. Sibille, Crystal-field states and defect levels in candidate quantum spin ice $Ce_2Hf_2O_7$, Phys. Rev. Mater. **6**, 044406 (2022).

[18] M. Hosoi, E. Z. Zhang, A. S. Patri, and Y. B. Kim, Uncovering Footprints of Dipolar-Octupolar Quantum Spin Ice from Neutron Scattering Signatures, Phys. Rev. Lett. **129**, 097202 (2022).

[19] S. Simon, A. S. Patri, and Y. B. Kim, Ultrasound detection of emergent photons in generic quantum spin ice, Phys. Rev. B **106**, 064427 (2022).

[20] A. S. Patri, M. Hosoi, and Y. B. Kim, Distinguishing dipolar and octupolar quantum spin ices using contrasting magnetostriction signatures, Phys. Rev. Res. **2**, 023253 (2020).

[21] O. Benton, Ground-state phase diagram of dipolar-octupolar pyrochlores, Phys. Rev. B **102**, 104408 (2020).

[22] A. Bhardwaj, S. Zhang, H. Yan, R. Moessner, A. H. Nevidomskyy, and H. J. Changlani, Sleuthing out exotic quantum spin liquidity in the pyrochlore magnet $Ce_2Zr_2O_7$, npj Quantum Mater. **7**, 51 (2022).

[23] X.-G. Wen, *Quantum Field Theory of Many-Body Systems: From the Origin of Sound to an Origin of Light and Electrons* (Oxford University Press, Oxford, 2007).

[24] L. Savary and L. Balents, Coulombic Quantum Liquids in Spin-1/2 Pyrochlores, Phys. Rev. Lett. **108**, 037202 (2012).

[25] G. Chen and L. Balents, Spin-orbit effects in $Na_4Ir_3O_8$: A hyper-kagome lattice antiferromagnet, Phys. Rev. B **78**, 094403 (2008).

[26] Y.-D. Li, X. Wang, and G. Chen, Hidden multipolar orders of dipole-octupole doublets on a triangular lattice, Phys. Rev. B **94**, 201114(R) (2016).

[27] C. Liu, Y.-D. Li, and G. Chen, Selective measurements of intertwined multipolar orders: Non-kramers doublets on a triangular lattice, Phys. Rev. B **98**, 045119 (2018).

[28] Y. Shen, C. Liu, Y. Qin, S. Shen, Y.-D. Li, R. Bewley, A. Schneidewind, G. Chen, and J. Zhao, Intertwined dipolar and multipolar order in the triangular-lattice magnet $TmMgGaO_4$, Nature Commun. **10**, 4530 (2019).

[29] C. Liu, C.-J. Huang, and G. Chen, Intrinsic quantum Ising model on a triangular lattice magnet $TmMgGaO_4$, Phys. Rev. Res. **2**, 043013 (2020).

[30] E. M. Smith, J. Dudemaine, B. Placke, R. Schafer, D. R. Yahne, T. DeLazzer, A. Fitterman, J. Beare, J. Gaudet, C. R. C. Buhariwalla, A. Podlesnyak, G. Xu, J. P. Clancy, R. Movshovich, G. M. Luke, K. A. Ross, R. Moessner, O. Benton, A. D. Bianchi, and B. D. Gaulin, Quantum spin ice response to a magnetic field in the dipole-octupole pyrochlore $Ce_2Zr_2O_7$, Phys. Rev. B **108**, 054438 (2023).

[31] R. Sibille, N. Gauthier, H. Yan, M. C. Hatnean, J. Ollivier, B. Winn, U. Filges, G. Balakrishnan, M. Kenzelmann, N. Shannon, and T. Fennell, Experimental signatures of emergent quantum electrodynamics in $Pr_2Hf_2O_7$, Nature Phys. **14**, 711 (2018).

[32] R. Sibille, E. Lhotel, M. C. Hatnean, G. Balakrishnan, B. Fåk, N. Gauthier, T. Fennell, and M. Kenzelmann, Candidate quantum spin ice in the pyrochlore $Pr_2Hf_2O_7$, Phys. Rev. B **94**, 024436 (2016).

[33] S. Petit, E. Lhotel, S. Guitteny, O. Florea, J. Robert, P. Bonville, I. Mirebeau, J. Ollivier, H. Mutka, E. Ressouche, C. Decorse, M. Ciomaga Hatnean, and G. Balakrishnan, Antiferroquadrupolar correlations in the quantum spin ice candidate $Pr_2Zr_2O_7$, Phys. Rev. B **94**, 165153 (2016).

[34] J.-J. Wen, S. M. Koohpayeh, K. A. Ross, B. A. Trump, T. M. McQueen, K. Kimura, S. Nakatsuji, Y. Qiu, D. M. Pajerowski, J. R. D. Copley, and C. L. Broholm, Disordered Route to the Coulomb Quantum Spin Liquid: Random Transverse Fields on Spin Ice in $Pr_2Zr_2O_7$, Phys. Rev. Lett. **118**, 107206 (2017).

[35] H. R. Molavian, M. J. P. Gingras, and B. Canals, Dynamically Induced Frustration as a Route to a Quantum Spin Ice State in $Tb_2Ti_2O_7$ via Virtual Crystal Field Excitations and Quantum Many-Body Effects, Phys. Rev. Lett. **98**, 157204 (2007).

[36] G. Chen, magnetic monopole condensation of the pyrochlore ice U(1) quantum spin liquid: Application to $Pr_2Ir_2O_7$ and $Yb_2Ti_2O_7$, Phys. Rev. B **94**, 205107 (2016).

[37] G. Chen, Dirac's "magnetic monopoles" in pyrochlore ice $U(1)$ spin liquids: Spectrum and classification, Phys. Rev. B **96**, 195127 (2017).

[38] Z. Liu, X. Zou, J.-W. Mei, and F. Liu, Selectively doping barlowite for quantum spin liquid: A first-principles study, Phys. Rev. B **92**, 220102(R) (2015).